

Synthesis and Structural Characterization of a Non-Heme Iron Hyponitrite Complex

Michael O. Lengel, Hai T. Dong, and Nicolai Lehner*

Department of Chemistry, The University of Michigan, Ann Arbor, Michigan 48109-1055

Supporting Information Placeholder

ABSTRACT: Flavodiiron NO reductases (FNORs) are important enzymes in microbial pathogenesis, as they equip microbes with resistance to the human immune defense agent nitric oxide (NO). Despite many efforts, intermediates that would provide insight into how the non-heme diiron active sites of FNORs reduce NO to N₂O could not be identified. Computations predict that iron-hyponitrite complexes are the key species, leading from NO to N₂O. However, the coordination chemistry of non-heme iron centers with hyponitrite is largely unknown. In this study, we report the reactivity of two non-heme iron complexes with preformed hyponitrite. In the case of [Fe(TPA)(CH₃CN)₂](OTf)₂, cleavage of hyponitrite and formation of an Fe₂(NO)₂ diamond core is observed. With less Lewis-acidic [Fe₂(BMPA-PhO)₂(OTf)₂] (2), reaction with Na₂N₂O₂ in polar aprotic solvent leads to the formation of a red complex, 3. X-ray crystallography shows that 3 is a tetranuclear iron-hyponitrite complex, [{Fe₂(BMPA-PhO)₂}_₂(μ-N₂O₂)](OTf)₂, with a unique hyponitrite binding mode. This species provided the unique opportunity to us to study the interaction of hyponitrite with non-heme iron centers and the reactivity of the bound hyponitrite ligand. Here, either protonation or oxidation of 3 is found to induce N₂O formation, supporting the hypothesis that hyponitrite is a viable intermediate in NO reduction.

Nitric oxide (NO) reduction is an important reaction in biology for various functions in the global nitrogen cycle. For example, in the denitrification pathway, which is a major microbial process that is responsible for large scale N₂O generation from agriculture, bacterial NO reductases (cNORs) reduce NO to N₂O, following the general equation:



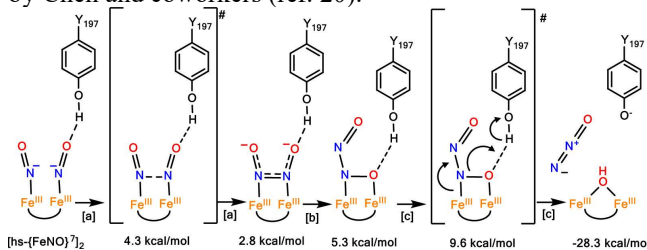
These bacterial NORs contain a heme cofactor and a non-heme iron center in the active site that can bind NO and carry out its reduction to N₂O.¹⁻³ More recently, it was discovered that certain flavodiiron proteins (FDPs) can act as potent NORs (flavodiiron NO reductases, FNORs).³⁻⁶ In these en-

zymes, a non-heme diiron active site carries out NO reduction, without the need for a heme cofactor to mediate the reaction. FNORs are found in pathogens (e.g. *Escherichia coli*, *Trichomonas vaginalis*, etc.) and are used as a defense system against the human immune defense agent NO.³ Here, a transcription factor senses NO and subsequently induces transcription of FNORs as a response to nitrosative stress.^{3,7,8} These enzymes mitigate NO toxicity by converting NO to less toxic N₂O, following eqn 1. As a result, harmful pathogens can survive and proliferate in the human body, causing chronic infections. Because of this, FNORs are potential targets for development of new antimicrobial agents.

The exact mechanism by which FNORs carry out NO reduction is still under intense investigation.⁹ Note that in the following, we use the Enemark-Feltham notation,¹⁰ {FeNO}ⁿ, where the exponent *n* corresponds to the number of valence (= Fe(d) + NO(π*)) electrons of the complex. Experimental studies on FNORs show NO binding to the diferrous active site of these enzymes, generating a [hs-{FeNO}⁷]₂ adduct as the catalytically competent intermediate (Scheme 1; hs = high-spin indicates that iron is in the hs state).^{11,12} Note that hs-{FeNO}⁷ complexes have an electronic structure that is best described as Fe(III)-NO⁻, reflecting NO's non-innocent properties as a ligand.³ Unfortunately, even when rapid freeze-quench methods are used, no intermediate of NO reduction could be trapped in FNORs past the [hs-{FeNO}⁷]₂ complex, and only formation of the oxidized (ferric) diiron core and N₂O was observed in these experiments.^{11,12} The same is true in synthetic (functional) complexes that model the chemistry of FNORs.¹³⁻¹⁹

Because of this lack of mechanistic insight, theoretical investigations have been used both for FNORs and a model complex to fill this void,²⁰⁻²² and identify relevant intermediates that lead from the [hs-{FeNO}⁷]₂ adduct to the formation of N₂O. Density functional theory (DFT) studies have identified iron-hyponitrite (N₂O₂²⁻) complexes as the key intermediates in the mechanism of NO reduction by FNORs. Here, N-N bond formation from the dinitrosyl adduct leads to the generation of an N-bound, bridging hyponitrite as the first intermediate (Scheme 1). This step is followed by rearrangement of the hyponitrite binding mode, with several possible structures of quite similar energies identified by theory, and ultimately N₂O release. Similarly, in cNORs, bridging hyponitrite intermediates have been proposed based on DFT calculations.^{3,23}

Scheme 1. Direct coupling mechanism for FNORs proposed by Chen and coworkers (ref. 20).^a



^a Energies indicated in the figure are relative to the starting [hs- $\{FeNO\}^7\]_2$ complex. Boxed letters correspond to reaction steps ([a]: N-N bond formation; [b]: hyponitrite isomerization; [c]: N-O bond cleavage). Transition states are indicated in brackets. Reprinted with Permission from ref. 3. Copyright 2021 American Chemical Society.

However, other than these theoretical predictions, not much is known *experimentally* about the coordination chemistry of non-heme iron centers with hyponitrite. Because of this lack of knowledge, no experimental guidelines exist that would allow scientists to identify suitable hyponitrite binding modes and link them via their electronic properties to reactivity, especially with respect to N_2O release. In fact, hyponitrite complexes of iron are generally rare, and only two examples have been reported to date that are structurally characterized, one utilizing heme centers²⁴ and the other one featuring dinitrosyl iron complexes (Figure 1).²⁵

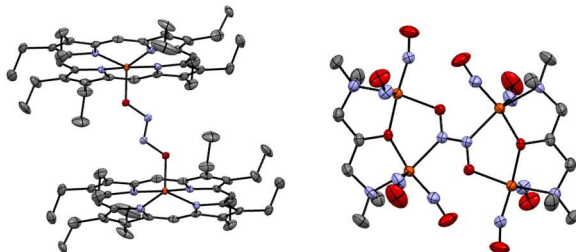
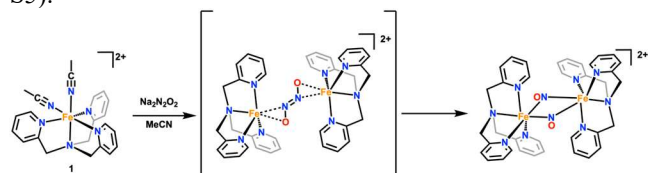


Figure 1. Crystal structure representations of the two reported Fe-hyponitrite complexes in the literature with ellipsoids drawn at 50% probability. Solvent molecules and hydrogen atoms are omitted for clarity. Fe atoms are colored in orange, oxygen in red, nitrogen in blue, and carbon in gray.

The goal of this study was to explore the biologically relevant coordination chemistry of hyponitrite with *non-heme* iron centers. In particular, we report the first structural characterization of a unique non-heme iron-hyponitrite complex, prepared from the ferrous precursor $[Fe^{II}_2(BMPA-PhO)_2(OTf)_2]$. Our results again underline the plasticity and versatility of hyponitrite as a ligand, which is able to interact with metal centers both through its N- and O-atoms, with the potential to form a multitude of bridging structures. In addition, we show that based on the Lewis-acidity of the iron centers, different reactions with hyponitrite are observed.

To explore the coordination chemistry of non-heme iron complexes and hyponitrite, we first reacted the complex

$[Fe^{II}(TPA)(MeCN)](X)_2$ (**1**, TPA = tris(methylpyridyl)-amine, X = OTf^- or PF_6^-) with commercially available sodium *trans*-hyponitrite \bullet x-hydrate ($Na_2N_2O_2 \bullet x$ -hydrate) in methanol (MeOH). Combining these reagents led to an immediate color change of the solution from orange to red, accompanied by a shift of the absorption band of **1-OTf** at 380 nm to 444 nm (Figure S12). The product of this reaction was then isolated and crystallized from a saturated acetonitrile (MeCN) solution at room temperature. X-ray crystallography revealed the dimeric complex $[Fe_2(TPA)_2(OMe)_2](OTf)_2$ with bridging methoxides as the reaction product (Figure S21). We hypothesized that hyponitrite reacts with MeOH to form N_2O , H_2O and methoxide under these conditions (Schemes S1-S2). To test this hypothesis, we quantified the amount of N_2O formed with $Na_2N_2O_2$ in methanol with and without **1** present and found N_2O formation for both (Table S1), in agreement with hyponitrite decomposition in MeOH. To address this problem, we changed the solvent to MeCN. Note that reactions with $Na_2N_2O_2 \bullet x$ -hydrate (or the anhydrous form) in MeCN are generally heterogeneous, as the salt does not dissolve in MeCN. Reaction of **1-OTf** with anhydrous $Na_2N_2O_2$ in MeCN over the course of 3 weeks gave a new product (in the presence of large amounts of starting material), which was characterized by X-ray crystallography and IR spectroscopy. To our surprise, this product corresponds to the previously reported complex $[Fe_2(TPA)_2(NO)_2](OTf)_2$, which features a $Fe_2(NO)_2$ diamond core structure. Here, two low-spin (ls) Fe(II) centers are bridged by two singlet NO^- ligands.²⁶ We hypothesized that hyponitrite indeed binds to two molecules of **1**, but that instead of forming a stable hyponitrite complex, the N=N bond is broken due to the strong Lewis acidity of the Fe(II) centers in **1**. To test whether the two bridging NO^- ligands indeed come from the same hyponitrite molecule, we performed an isotopic scrambling experiment where **1** was reacted with a 1:1 mixture of anhydrous $Na_2N_2O_2$ and $Na_2^{15}N_2O_2$. Figure S10 shows the IR spectrum of the product isolated from this reaction, which demonstrates that only the unlabeled $Fe_2(NO)_2$ and fully-labeled $Fe_2(^{15}NO)_2$ products have formed, but no isotope scrambling occurred. These results show that hyponitrite is cleaved *intramolecularly* after binding to two molecules of **1-OTf** (Scheme 2), indicating that the Lewis-acidity of the ferrous iron centers is an important parameter that needs to be controlled in order to allow for the formation and stabilization of hyponitrite intermediates. DFT calculations support these conclusions, showing that the N-O stretching frequency of a scrambled $^{14}NO-^{15}NO$ product falls right in-between those of the $^{14}N-^{14}N$ and $^{15}N-^{15}N$ complexes (Table S5).



Scheme 2. Schematic representation of the *intramolecular* hyponitrite cleavage upon the reaction of **1-OTf** with anhydrous $Na_2N_2O_2$.

The fact that the Fe(TPA) unit is highly Lewis-acidic is evident from the corresponding NO complex, $[\text{Fe}(\text{TPA})(\text{OTf})(\text{NO})](\text{OTf})$, which has an N-O stretching frequency $>1800 \text{ cm}^{-1}$, which is at the upper end of N-O stretches observed for $\text{hs}\text{-}\{\text{FeNO}\}^7$ complexes.²⁶⁻²⁸ Note that these species generally have Fe(III)-NO⁻ type electronic structures. Here, the highly Lewis-acidic iron center receives strong electron donation from the $^3\text{NO}^-$ ligand, causing the high-energy N-O stretching mode.³ To tame the Lewis-acidity of the Fe(TPA) system, we replaced one of the neutral pyridine donors in TPA with a strongly donating, anionic phenolate group. The corresponding ligand BMPA-PhOH (2-((bis(pyridin-2-ylmethyl)amino)methyl)phenol; Figure S1) was synthesized using a modified literature procedure.¹⁷ Metallations were generally carried out either by in-situ deprotonation of BMPA-PhOH using KOMe in MeOH or from the corresponding Li[BMPA-PhO] salt. When Li[BMPA-PhO] is reacted with 1 equiv. $[\text{Fe}(\text{OTf})_2 \cdot 2\text{MeCN}]$ in THF, a bright yellow solid precipitates from solution. After washing with THF, pure complex **2** is obtained. Single crystals suitable for X-ray diffraction were grown by slow diffusion of diethyl ether into a saturated solution of **2** in MeCN at room temperature, yielding yellow rods. The crystal structure reveals that complex **2** is a dimer with the two iron centers bridged by the O-atoms of the phenolate arms of the BMPA-PhO⁻ ligands, forming a diamond core (Figure 2). The Fe-O distances in the core are 2.01 and 2.04 Å for the short bonds and 2.15 and 2.16 Å for the longer bonds. Therefore, this core is quite asymmetric. The two iron centers are separated by 3.26 Å and they both have a pseudo-octahedral geometry completed by the coordination of a triflate counter anion. This Fe-Fe separation compares well to FNORs,³ indicating that complex **2** is a suitable structural model for the active sites of these enzymes, and a good starting point to explore the hyponitrite reactivity of diiron complexes.

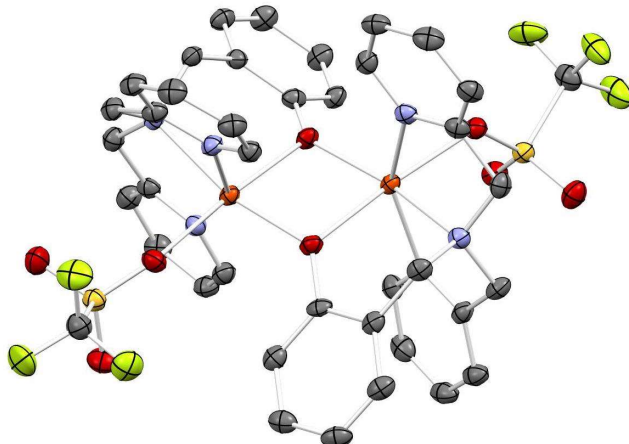


Figure 2. Crystal structure of complex $[\text{Fe}_2(\text{BMPA-PhO})_2(\text{OTf})_2]$ (**2**) with ellipsoids drawn at 50% probability. Solvent molecules and hydrogen atoms are omitted for clarity. Fe atoms are colored in orange, oxygen in red, nitrogen in blue, carbon in gray, sulfur in yellow, and fluorine in lime-green.

Reaction of complex **2** with $\text{Na}_2\text{N}_2\text{O}_2 \cdot x\text{-hydrate}$ in MeCN at 25 °C overnight led to a color change of the solution from yellow to deep red. Upon workup, **3-OTf** was obtained as a red-orange powder. Slow diffusion of diethyl ether into a MeCN solution of **3-OTf** then yielded orange plates suitable for X-ray crystallography. The crystal structure of **3-OTf** reveals a unique dimerization of two molecules of **2** to form a tetra-iron complex, $[\{\text{Fe}_2(\text{BMPA-PhO})_2\}_2(\mu\text{-N}_2\text{O}_2)](\text{OTf})_2$, with hyponitrite bridging the two diiron cores as shown in Figure S23. A salt metathesis of **2** with NaBArF (BArF = tetrakis(3,5-bis(trifluoromethyl)phenyl)borate), followed by addition of $\text{Na}_2\text{N}_2\text{O}_2 \cdot x\text{-hydrate}$, led to the formation of **3-BArF**. The crystal structure of **3-BArF** shows the same tetranuclear iron complex as **3-OTf**, except with BArF counter ions. The crystal structure of **3-BArF** is of higher quality than that of **3-OTf** and is therefore shown in Figure 3. Interestingly, the hyponitrite ion is bound to the four iron centers in the tetramer by both of its N- and O-atoms, which represents a unique binding mode that has not been observed before, as illustrated in Scheme 3. In this binding mode, each diiron unit is bound to an O- and an N-atom of hyponitrite. The N-N bond distance of hyponitrite is 1.26 Å, which represents an N=N double bond. This is identical to the N=N bond distance in $\text{Na}_2\text{N}_2\text{O}_2$ (1.26 Å).²⁹ The average N-O bond distance of the hyponitrite ligand in **3** is 1.36 Å, again identical to $\text{Na}_2\text{N}_2\text{O}_2$ (1.36 Å). The same is true for the N-N-O bond angle (**3**: 114°; $\text{Na}_2\text{N}_2\text{O}_2$: 112°). Hence, despite the coordination of hyponitrite to four iron centers in the tetramer, the ligand does not seem activated. This supports the mechanistic conclusions from Chen and coworkers²⁰ where it was proposed that protonation is necessary in order to activate the bound

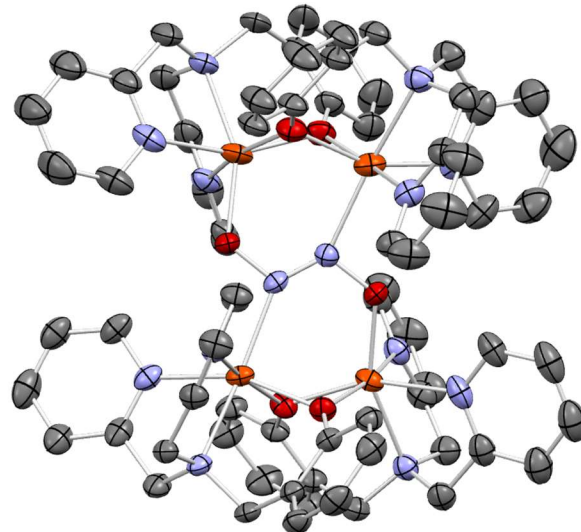
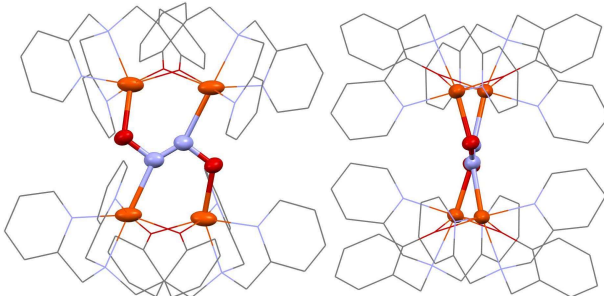


Figure 3. Crystal structure of complex $[\{\text{Fe}_2(\text{BMPA-PhO})_2\}_2(\mu\text{-N}_2\text{O}_2)](\text{BArF})_2$ (**3-BArF**) with ellipsoids drawn at 50% probability. The BArF counter anions, solvent molecules, and hydrogen atoms are omitted for clarity. Fe atoms are colored in orange, oxygen in red, nitrogen in blue, and carbon in gray.

hyponitrite ligand in FNORs for N_2O generation. Finally, the average Fe-N and Fe-O distances are 2.21 and 2.00 Å, re-

spectively, which indicates that the Fe-O bond is distinctively stronger than the Fe-N bond. Based on this observation, we conclude that hyponitrite prefers O-coordination over N-coordination to non-heme iron centers. This supports the mechanistic proposal for FNORs that N-N bond formation, which leads to the generation of a bridging, N-bound hyponitrite ligand, is immediately followed by hyponitrite rearrangement from N- to N,O-coordination, as shown in Scheme 1.



Scheme 3. Schematic representation of the crystal structure of **3**, emphasizing the bridging hyponitrite binding mode.

Complex **3** has a diamagnetic ground state based on low temperature MCD data (Figure S18). Previous studies have shown that hyponitrite does not mediate magnetic exchange coupling,³⁰ however, our DFT calculations predict that exchange coupling may occur through the hyponitrite bridge in **3** (Figure S20). Finally, IR spectroscopy revealed a new feature at $\sim 1070\text{ cm}^{-1}$ for **3-OTf**, characteristic of the N-O stretch of hyponitrite. This assignment was confirmed by isotope labeling (see Figure S11).

The possibility of activating the bound hyponitrite in **3** by protonation was further tested by adding Brookhart's acid (H₂ArF) as a proton source to a solution of **3-OTf**. Interestingly, with 1 equiv. of acid, only about 6% N₂O formation is observed. Addition of 5 equiv.s of acid are required for quantitative N₂O formation (Figure 4). We postulate that the extra equiv.s of acid are required for N₂O generation because phenolates are protonated before the hyponitrite unit, thus leading to depressed N₂O yields with less than 5 equiv.s of acid. To further investigate how the Lewis-acidity of iron plays a key role in the stability of hyponitrite complexes, N₂O yields were determined after oxidation of **3-OTf**. These results show quantitative N₂O formation when two equiv.s of oxidant are used (Table S4). Upon oxidation from the ferrous to the ferric state, the iron centers become more Lewis-

acidic, promoting N₂O formation by hyponitrite decomposition.

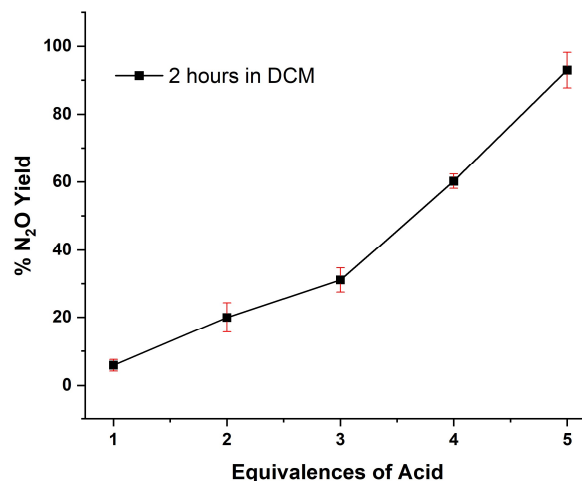


Figure 4. N₂O yields obtained by adding different equivalences of H₂ArF to a solution of **3-OTf** in dichloromethane.

In summary, this work provides key insight into the properties of hyponitrite complexes of non-heme iron centers. First, we show that the Lewis acidity of the Fe(II) center, which is easily gauged by the N-O stretching frequency of the corresponding hs- $\{\text{FeNO}\}^7$ complexes, is a key feature that determines the stability of the hyponitrite complexes. To our surprise, iron centers that are too Lewis-acidic promote cleavage of hyponitrite into two NO⁻ units, followed by further reactions (in the case of the Fe(TPA) unit, this is formation of a unique Fe₂(NO)₂ structure). Taming the iron centers to make them less Lewis-acidic allowed for the isolation of a unique, tetrameric hyponitrite complex, where hyponitrite bridges between two dimeric Fe₂(BMPA-PhO)₂ units. This complex was structurally characterized, and shows that hyponitrite has a preference to bind to the non-heme iron centers via its O atoms. This result supports mechanistic proposals for FNORs that after hyponitrite formation, the ligand would quickly rotate from an N- to an N,O-coordination mode. Finally, upon addition of 5 equivalences of acid to our tetrameric hyponitrite complex, quantitative N₂O formation is observed, indicating that protonation is key for hyponitrite activation and N₂O formation. Similarly, N₂O formation can be induced by oxidation of the complex.

ASSOCIATED CONTENT

Supporting Information

Synthetic procedures; UV-Visible, IR, NMR, CV data, mass spectrometry, and DFT optimized coordinates. This material is available free of charge via the Internet at <http://pubs.acs.org>. Supplementary crystallographic data can be found at CCDC deposition 2084197, 2084198, 2084199, and 2357265 and can be obtained free of charge.

AUTHOR INFORMATION

Corresponding Author

Lehnertn@umich.edu
twitter: @UMLehnertgroup

Notes

The authors declare no competing financial interest.

ACKNOWLEDGMENT

This work was supported by the National Science Foundation (CHE-2002885 to NL). We acknowledge Dr. Jeff

Kampf (University of Michigan) for X-ray crystallographic analysis of complex **2** and **3-OTf**, and Dr. Fengrui Qu (University of Michigan) for solving the crystal structure of **3-BArF**. We further acknowledge funding from NSF grant CHE-0840456 for X-ray instrumentation.

REFERENCES

1. Watmough, N. J.; Field, S. J.; Hughes, R. J. L.; Richardson, D. J. The Bacterial Respiratory Nitric Oxide Reductase. *Biochem. Soc. Trans.* **2009**, *37*, 392-399.
2. Wasser, I. M.; de Vries, S.; Moënne-Loccoz, P.; Schröder, I.; Karlin, K. D. Nitric Oxide in Biological Denitrification: Fe/Cu Metalloenzymes and Metal Complex NO_x Redox Chemistry. *Chem. Rev.* **2002**, *102*, 1201-1234.
3. Lehnert, N.; Kim, E.; Dong, H. T.; Harland, J. B.; Hunt, A. P.; Manickas, E. C.; Oakley, K. M.; Pham, J.; Reed, G. C.; Sosa Alfaro, V. The Biologically Relevant Coordination Chemistry of Iron and Nitric Oxide: Electronic Structure and Reactivity. *Chem. Rev.* **2021**, *121*, 14682-14905.
4. Romão, C. V.; Vicente, J. B.; Borges, P. T.; Frazão, C.; Teixeira, M. The Dual Function of Flavodiiron Proteins: Oxygen and/or Nitric Oxide Reductases. *J. Bio. Inorg. Chem.* **2016**, *21*, 39-52.
5. Khatua, S.; Majumdar, A. Flavodiiron Nitric Oxide Reductases: Recent Developments in the Mechanistic Study and Model Chemistry for the Catalytic Reduction of NO. *J. Inorg. Biochem.* **2015**, *142*, 145-153.
6. Kurtz, D. M., Jr. Flavo-Diiron Enzymes: Nitric Oxide or Dioxygen Reductases? *Dalton Trans.* **2007**, 4115-4121.
7. Gardner, A. M.; Helmick, R. A.; Gardner, P. R. Flavorubredoxin, an Inducible Catalyst for Nitric Oxide Reduction and Detoxification in *Escherichia coli*. *J. Biol. Chem.* **2002**, *277*, 8172-8177.
8. Gardner, A. M.; Gessner, C. R.; Gardner, P. R. Regulation of the Nitric Oxide Reduction Operon (*norRVW*) in *Escherichia coli*. Role of NorR and β^{54} in the Nitric Oxide Stress Response. *J. Biol. Chem.* **2003**, *278*, 10081-10086.
9. Lehnert, N.; Fujisawa, K.; Camarena, S.; Dong, H. T.; White, C. J. Activation of Non-Heme Iron-Nitrosyl Complexes: Turning up the Heat. *ACS Catal.* **2019**, *9*, 10499-10518.
10. Enemark, J. H.; Feltham, R. D. Principles of Structure, Bonding, and Reactivity for Metal Nitrosyl Complexes. *Coord. Chem. Rev.* **1974**, *13*, 339-406.
11. Caranto, J. D.; Weitz, A.; Giri, N.; Hendrich, M. P.; Kurtz, D. M., Jr. A Diferrous-Dinitrosyl Intermediate in the N₂O-Generating Pathway of a Deflavinated Flavo-Diiron Protein. *Biochemistry* **2014**, *53*, 5631-5637.
12. Caranto, J. D.; Weitz, A.; Hendrich, M. P.; Kurtz, D. M., Jr. The Nitric Oxide Reductase Mechanism of a Flavo-Diiron Protein: Identification of Active-Site Intermediates and Products. *J. Am. Chem. Soc.* **2014**, *136*, 7981-7992.
13. Dong, H. T.; White, C. J.; Zhang, B.; Krebs, C.; Lehnert, N. Non-Heme Diiron Model Complexes Can Mediate Direct NO Reduction: Mechanistic Insight into Flavodiiron NO Reductases. *J. Am. Chem. Soc.* **2018**, *140*, 13429-13440.
14. Jana, M.; Pal, N.; White, C. J.; Kupper, C.; Meyer, F.; Lehnert, N.; Majumdar, A. Functional Mononitrosyl Diiron(II) Complex Mediates the Reduction of NO to N₂O with Relevance for Flavodiiron NO Reductases. *J. Am. Chem. Soc.* **2017**, *140*, 14380-14383.
15. Jana, M.; White, C. J.; Pal, N.; Demeshko, S.; Meyer, F.; Lehnert, N.; Majumdar, A. Functional Models for the Mono- and Dinitrosyl Intermediates of FNORs: Semireduction versus Superreduction of NO. *J. Am. Chem. Soc.* **2020**, *142*, 6600-6616.
16. White, C. J.; Speelman, A. L.; Kupper, C.; Demeshko, S.; Meyer, F.; Shanahan, J. P.; Alp, E. E.; Hu, M.; Zhao, J.; Lehnert, N. The Semireduced Mechanism for Nitric Oxide Reduction by Non-Heme Diiron Complexes: Modeling Flavodiiron Nitric Oxide Reductases. *J. Am. Chem. Soc.* **2018**, *140*, 2562-2574.
17. Zheng, S.; Berto, T. C.; Dahl, E. W.; Hoffman, M. B.; Speelman, A. L.; Lehnert, N. The Functional Model Complex [Fe₂(BPMP)(OPr)(NO)₂](BPh₄)₂ Provides Insight into the Mechanism of Flavodiiron NO Reductases. *J. Am. Chem. Soc.* **2013**, *135*, 4902-4905.
18. White, C. J.; Lengel, M. O.; Bracken, A. J.; Kampf, J. W.; Speelman, A. L.; Alp, E. E.; Hu, M. Y.; Zhao, J.; Lehnert, N. Distortion of the [FeNO]₂ Core in Flavodiiron Nitric Oxide Reductase Models Inhibits N-N Bond Formation and Promotes Formation of Unusual Dinitrosyl Iron Complexes: Implications for Catalysis and Reactivity. *J. Am. Chem. Soc.* **2022**, *144*, 3804-3820.
19. Dong, H. T.; Zong, Y.; Bracken, A. J.; Lengel, M. O.; Kampf, J. W.; Sil, D.; Krebs, C.; Lehnert, N. Synthesis and characterization of a model complex for flavodiiron NO reductases that stabilizes a diiron mononitrosyl complex. *J. Inorg. Biochem.* **2022**, *229*, 111723.

20. Lu, J.; Bi, B.; Lai, W.; Chen, H. Origin of Nitric Oxide Reduction Activity in Flavo-Diiron NO Reductase: Key Roles of the Second Coordination Sphere. *Angew. Chem. Int. Ed.* **2019**, *58*, 3795-3799.

21. Van Stappen, C.; Lehnert, N. Mechanism of N-N Bond Formation by Transition Metal-Nitrosyl Complexes: Modeling Flavodiiron Nitric Oxide Reductases. *Inorg. Chem.* **2018**, *57*, 4252-4269.

22. Blomberg, M. R. A.; Ädelroth, P. Reduction of Nitric Oxide to Nitrous Oxide in Flavodiiron Proteins: Catalytic Mechanism and Plausible Intermediates. *ACS Catal.* **2023**, *13*, 2025-2038.

23. Blomberg, M. R. A. Can Reduction of NO to N₂O in Cytochrome *c* Dependent Nitric Oxide Reductase Proceed through a Trans-Mechanism? *Biochemistry* **2017**, *56*, 120-131.

24. Xu, N.; Campbell, A. L. O.; Powell, D. R.; Khandogin, J.; Richter-Addo, G. B. A Stable Hyponitrite-Bridged Iron Porphyrin Complex. *J. Am. Chem. Soc.* **2009**, *131*, 2460-2461.

25. Wu, W.-Y.; Hsu, C.-N.; Hsieh, C.-H.; Chiou, T.-W.; Tsai, M.-L.; Chiang, M.-H.; Liaw, W.-F. NO-to-[N₂O₂]²⁻-to-N₂O Conversion Triggered by {Fe(NO)₂}¹⁰⁻-{Fe(NO)₂}⁹⁻ Dinuclear Dinitrosyl Iron Complex. *Inorg. Chem.* **2019**, *58*, 9586-9591.

26. Dong, H. T.; Speelman, A. L.; Kozemchak, C. E.; Sil, D.; Krebs, C.; Lehnert, N. The Fe₂(NO)₂ Diamond Core: A Unique Structural Motif in Non-Heme Iron-NO Chemistry. *Angew. Chem. Int. Ed.* **2019**, *131*, 17859-17863.

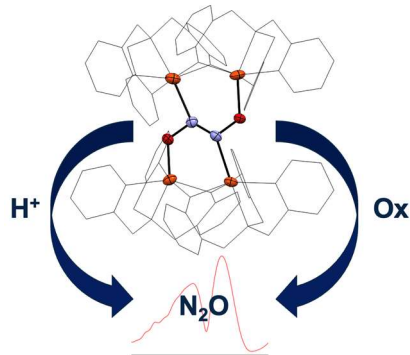
27. Li, J.; Banerjee, A.; Pawlak, P. L.; Brennessel, W. W.; Chavez, F. A. Highest Recorded N-O Stretching Frequency for 6-Coordinate {Fe-NO}⁷ Complexes: An Iron Nitrosyl Model for His₃ Active Sites. *Inorg. Chem.* **2014**, *53*, 5414-5416.

28. Pal, N.; Jana, M.; Majumdar, A. Reduction of NO by diiron complexes in relation to flavodiiron nitric oxide reductases. *Chem. Commun.* **2021**, *57*, 8682-8698.

29. Arulsamy, N.; Bohle, D. S.; Imonigie, J. A.; Sagan, E. S. Synthesis and Characterization of Alkylammonium Hyponitrites and Base-Stabilized Hyponitrous Acid Salts. *Inorg. Chem.* **1999**, *38*, 2716-2725.

30. Berto, T. C.; Xu, N.; Lee, S. R.; McNeil, A. J.; Alp, E. E.; Zhao, J.; Richter-Addo, G. B.; Lehnert, N. Characterization of the Bridged Hyponitrite Complex {[Fe(OEP)]₂(¹-N₂O₂)}: Reactivity of Hyponitrite Complexes and Biological Relevance. *Inorg. Chem.* **2014**, *53*, 6398-6414.

TOC figure:



Graphical Abstract: **Fe-Hyponitrite Reactivity:** The Fe-hyponitrite complex **3** was generated from pre-formed hyponitrite and characterized by spectroscopic methods and X-ray crystallography. Upon protonation or oxidation, quantitative N₂O formation occurs. Lewis acidity of iron plays a key role in reactivity, as a more Lewis acidic iron center leads to the cleavage of the N=N bond of hyponitrite.